Quality Inspection of Additive Construction: A Parametric Approach for Automated Scanning of 3D Printed Walls

Jorge Rojas[1] and Sogand Hasanzadeh[1]

[1]Lyles School of Civil and Construction Engineering, Purdue University, United States of America
rojas27@purdue.edu, sogandm@purdue.edu

Abstract –

Additive construction, also known as 3D concrete printing (3DCP), has emerged as a promising construction method with the potential to address industry challenges, such as low productivity and a shortage of skilled labor. In 3DCP, it is critical to have a reliable, realtime inspection process that continuously monitors material deposition, layer geometry, and interlayer bonding as the structure is being printed. The absence of such a process limits the ability to detect, interrupt, and correct defects in real time, thereby increasing the risk of geometric deviations and potentially compromising structural integrity. Vision-based inspection offers low cost and high accuracy at close range; however, existing approaches typically rely on cameras fixed to the printhead, limiting the field of view (FoV) to a local and instantaneous assessment of freshly extruded layers. This paper proposes a flexible FoV scanning workflow enabled by a mobile manipulator and a parametric modeling framework that dynamically updates the camera toolpath based on printing progress. The system maintains close proximity to the printed surface while significantly expanding the inspected area. Findings demonstrated that the proposed automated approach can (1) reduce human intervention for inspection, (2) achieve strong agreement between predicted and measured scanning coverage, and (3) increase by 13 and 4 times the inspection area compared to fixed- and printhead-mounted camera configurations, respectively. The proposed approach enables automated, flexible FoV inline scanning for 3DCP and provides a foundation for future vision-based quality assessment during printing.

Keywords –

Parametric Modeling; 3D Concrete Printing; Quality Inspection; Mobile Robot.

1 Introduction

The construction industry continues to face pressing challenges, including low productivity due to limited technology adoption, insufficient automation of construction processes, labor shortages, and an aging workforce [1]. In response, there is growing interest in innovative construction methods that enhance automation and productivity. Among these, 3D Concrete Printing (3DCP) has emerged as a promising solution, offering increased productivity through automation, reduced labor requirements, and the elimination of traditional formwork activities [2].

Despite these advantages, 3DCP presents significant technical challenges, particularly regarding the time-sensitive behavior of fresh cementitious materials during printing. Material properties evolve rapidly after extrusion, and variations in rheology and setting behavior can lead to quality defects that require immediate attention. Common defects reported in the literature include breakpoints [3], layer-geometry deformations, dry-material texture, and buildability collapse [4]. These defects often occur during printing and may compromise structural integrity if not detected in realtime.

Unlike additive manufacturing in traditional rapid prototyping—where quality inspection can typically be performed after fabrication during post-processing—additive construction (especially 3DCP) requires inline inspection systems capable of monitoring the material condition while it is still fresh. Currently, inline quality monitoring in 3DCP is predominantly performed by human operators through visual inspection. Recently, however, a wide range of sensing technologies has been explored for inline inspection in 3DCP, including PZT patches [5], 2D and 3D cameras, 1D/2D/3D laser sensors, terrestrial laser scanners, structured-light scanners [6], and 2D LiDAR systems [7]. Among these options, 2D imaging sensors have emerged as particularly promising due to their affordability, high spatial resolution, and suitability for close-range monitoring.

However, the effectiveness of 2D imaging systems is constrained by their limited field of view (FoV) when placed in close proximity to the printed material. A review of existing studies reveals that most laboratory-scale implementations rely on cameras mounted on tripods or rigidly attached to the printhead, providing fixed top- or lateral-view image of the most recently deposited layers [6]. As a result, current inline inspection approaches are restricted to narrow or fixed FoV, enabling monitoring only of the immediate vicinity of the extrusion path. This limitation prevents comprehensive observation of material behavior across the broader 3D-printed structure, highlighting a critical gap in the existing literature. Thus, this paper proposes a parametric modeling framework that enables a mobile robotic system to achieve a flexible FoV, dynamically updating the camera scanning motion based on the printing progress.

2 Background

2.1 Inline Inspection of Material Behavior

There are two main properties critical to the quality monitoring of 3DCP elements: extrudability and buildability. Extrudability is related to the continuity and level of defects on the printed surface, while buildability is associated with the geometry deformation in the printed layers [8]. Defects or issues associated with extrudability may involve filament breakpoints [3], overextrusion or underextrusion, which are visible as variations in layer width [9], or defects such as racks and notches [8]. On the other hand, characteristics associated with buildability may include layer settlements, reflected in surface texture and water loss [4], and layer deformation, reflected in their height, orientation, and curvature [9]. Previous studies have examined monitoring all these features using cameras as an economically and accurately viable alternative to inline inspection, placing cameras at different locations to capture top- or lateral-view images of the printed layers [6].

2.2 Inline Inspection with FoV

Previous studies have identified computer vision techniques based on camera sensors as among the most reliable and responsive approaches for monitoring material variations in 3DCP [10]. However, camera-based monitoring systems face several challenges, including sensitivity to focal distance and viewpoint, limited FoV, and image resolution expressed as pixels per millimeter (ppm) [6].

Among these factors, the FoV plays a critical role, as it directly influences other constraints. Strategic placement and planning of camera positions can expand the observable area, enable dynamic orientation, and maintain close proximity to the targeted surface, thereby improving measurement precision through higher ppm. Nevertheless, these objectives often involve trade-offs between coverage and resolution.

Several studies have adopted a fixed-camera configuration, mounted on a tripod at a sufficient distance to cover the area of interest (AoI), typically capturing a lateral view of the printed layers [4]. While this approach provides a global view of the printed structure, it requires the camera to be placed far from the print, which negatively affects image resolution and measurement accuracy.

An alternative configuration involves mounting the camera directly on the printhead, oriented perpendicularly to the printing bed to capture a top view of the freshly deposited layers [3]. However, due to the physical size of the printhead, the camera must be positioned very close to the material surface, resulting in a narrow FoV.

To address this limitation, two solutions have been proposed in the literature. The first involves using two cameras that alternated on the printing direction, ensuring that the freshly printed upper layer remains within the FoV [11]. The second solution employs a single camera mounted on a rotary mechanism, allowing dynamic adjustment of the FoV by changing the camera orientation relative to the printhead as the toolpath geometry varies [12]. Despite these improvements, both approaches still require close proximity to the printed surface and provide only a limited local FoV, restricting measurements primarily to local filament width.

A different top-view approach incorporates a 2D laser to emulate a structured-light scanning system. In this configuration, a laser line is projected onto the printed layer and the printing bed, enabling precise estimation of layer height from the offset between the projected lines [7]. While this method can achieve high accuracy, it is generally suitable only for single-layer measurements near the printing bed and for simple, planar toolpaths (2.5D printing), as more complex geometries would require frequent, significant changes in camera orientation.

To capture richer information about material behavior during printing, some studies have explored lateral-view cameras mounted on the printhead. This configuration typically uses a bracket offset from the printhead to capture an orthogonal side view of the top layers, enabling observation of extrudability behavior through surface defects such as cracks and notches, as well as layer height deviations related to settlement and buildability [8]. However, the protruding bracket limits the allowable distance between the camera and the printed surface, resulting in a narrow FoV focused only on the uppermost layers. Consequently, this approach cannot capture deformation or instability in lower layers, which are critical as they carry increasing loads from the layers above. In summary, existing methods predominantly focused on close-proximity, dynamically oriented views of upper layers, while neglecting lower layers that experience higher cumulative loads during printing.

3 Point of Departure

Camera-based computer vision systems are widely used for inline monitoring of material properties in 3DCP; however, their effectiveness is fundamentally constrained by the FoV. Existing approaches typically trade spatial coverage for precision, relying either on close-proximity views that capture only localized behavior of the uppermost layers or on distant, fixed viewpoints that reduce measurement accuracy. To address FoV limitations in camera-based 3DCP monitoring, this study proposes a unified inspection workflow that integrates (i) a parametric scanning toolpath generation method, (ii) mobile robotic manipulation for multi-view repositioning, and (iii) Digital Twin–based updating of the scanning trajectory according to printing progress. This combined approach expands the inspection AoI without sacrificing resolution by maintaining a controlled standoff distance and continuously adjusting camera pose relative to the printed toolpath. By decoupling FoV coverage from static camera placement, the method provides a broader and more informative visual context of the printed surface without sacrificing resolution, thereby enabling broader inline inspection across freshly printed upper layers and heavily loaded lower layers.

4 Methodology

4.1 Robotic System Integration

The proposed robotic system consists of a mobile manipulator composed of a UR5e mounted on a Husky A200 unmanned ground vehicle (UGV). The platform is equipped with a VLP-16 LiDAR and an inertial measurement unit (IMU), enabling SLAM-based localization and mapping. Navigation and motion control are implemented using A^* path planning and Pure Pursuit algorithms, following the framework described in [14].

The UR5e manipulator is equipped with an Intel RealSense D435i mounted near the end effector. The camera was calibrated in an eye-on-hand configuration using the *Tsai–Lenz* algorithm and a *ChArUco* marker to accurately define the transformation between the camera frame and the tool center point (TCP).

The mobile manipulator operates in coordination with an ABB IRB 6700 235/2.65 industrial robot, which serves as a 3D concrete printer. Communication between the robots is enabled through a local Wi-Fi network. To facilitate data collection in a dry laboratory environment, a virtual controller that simulates the physical printer was deployed in RobotStudio. The same robot application was overlaid at scale in the laboratory using RobotStudio AR on a tablet device. A digital replica of the system was developed in Rhino 7 and Grasshopper (GH), integrating the virtual printer, camera sensor, and mobile manipulator (Figure 1).

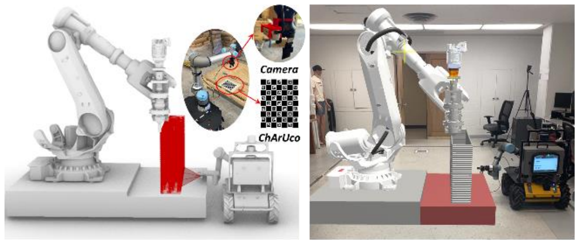

Grasshopper Digital Replica **AR Printer with Mobile Robot**

Figure 1. Grasshopper Digital Replica and Mobile Manipulator with RobotStudio AR 3D Printer

4.2 Camera Scanning Toolpath

The robotic system was designed to dynamically adjust the camera FoV based on the current printing height of the wall. The printing height is continuously updated using feedback from the 3D printer extruder position, transmitted from the RobotStudio virtual controller via Machina Bridge (MB) [15] and received within a GH script.

In scenarios involving multiple walls, such as building-scale 3D printing, the mobile robot autonomously navigates to predefined parking goals near each wall and refines its location by scanning a fiducial marker placed within the printer workspace.

A custom GH component was developed for marker detection, reading camera data streamed from a ROS node (Figure 2a). The refined robot pose is then updated within the Rhino 7 model relative to the printer coordinate reference system using another custom GH component (Figure 2b).

Based on the refined localization and current printing progress, a camera-scanning toolpath is generated using a parametric modeling approach. The toolpath GH component receives as inputs the camera's horizontal and vertical FoV angles, the distance to the wall surface, the desired vertical overlap between scanning paths, wall dimensions, and the UR5e's reachable limits. Although wall height is defined parametrically, it is dynamically updated during execution using realtime printer feedback (Figure 2c).

The scanning strategy follows a bottom-top sequence, with vertical steps equal to the camera vertical field of view (VFoV). At each height, the end effector follows the trajectory parallel to the wall surface while maintaining a constant standoff distance. Horizontal limits are defined as half the camera's horizontal field of view (HFoV) at each end of the wall. The total number of scanning passes is computed based on the dynamically updated wall height.

To visualize camera coverage, a GH component was developed to model the camera frustum as a BRep pyramid using the camera parameters (HFoV, VFoV, and depth distance), as shown in Figure 2d. The 3D printer toolpath was defined using a workflow presented in [16] and encapsulated in a GH component (Figure 2e). All components are integrated into a single GH script that serves as a parametric modeling hub linking the digital replica and the physical robotic system.

4.3 Parametric Modeling Hub

The robotic application enables a flexible FoV by dynamically adapting the camera scanning route to the current printing height extracted from the 3D printer toolpath. System integration is achieved through a parametric modeling hub implemented in GH, which communicates with the 3D printer controller via MB, the UGV via Rosbridge, and the UR5e via FTP protocols (Figure 2).

The 3DCP toolpath is first defined in GH and transmitted to the RobotStudio controller or its Rhino 7 digital replica for simulation. Feedback from the virtual controller is used to update the wall height in realtime, which drives the camera toolpath generation for the UR5e. The manipulator kinematics are simulated in GH prior to execution, and the resulting commands are sent to the physical robot. During simulation, the camera frustum (i.e., represents what a camera can see) is continuously updated based on the current camera pose.

A ROS-based task manager coordinates actions among the UGV, UR5e, and camera, including navigation to parking goals, marker scanning, localization refinement, and wall scanning. Marker detection results are transmitted back to GH to update the digital replica and adjust the camera toolpath before execution. This bidirectional data exchange enables continuous synchronization between the physical system and its digital counterpart, forming a digital replica that mimics appearance and behavior of the actual 3DCP process, also known as Digital Twin, which is further discussed in the next subsection.

4.4 Experimental Setup

The research develops a Digital Shadow scanning workflow prototype, which serves as a foundation for a broader DT framework for intelligent inline inspection in 3DCP, which is out of the scope of this paper. Within the scope of this study, the Digital Shadow implementation follows the seven-layer architecture presented by [17].

These layers include *physical*, *digital*, *sensing*, *perception*, *control*, *communication*, and *device/display* layers. Figure 3 illustrates the seven layers explicitly implemented to support flexible FoV scanning in this study.

In the current implementation, the *digital* replica serves as the central coordination layer that commands robot actions. Marker scanning is initiated as a *sensing* task, and the acquired camera data are used to compute refined coordinates of the mobile robot and manipulator through *perception*. These updated poses are then *communicated* back to the virtual environment, where the digital model is synchronized accordingly.

With the refined robot position embedded in the digital replica, a camera scanning toolpath is generated using a parametric modeling approach. The resulting routing commands are transmitted to the *physical* robotic system to execute the scanning motion (*control*), while the camera continuously acquires visual data from the 3D-printed wall (*sensing*). Although the proposed workflow is designed to support downstream integration with computer vision algorithms for surface analysis and closed-loop control of the 3D printing process (dimmed grey in Figure 3), the present research focuses specifically on enabling and validating a flexible camera-

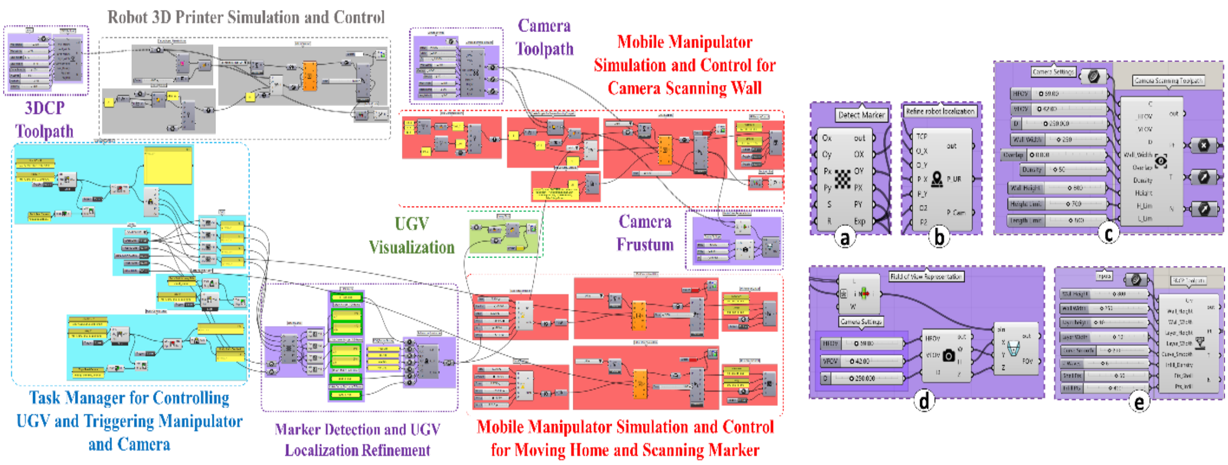

Figure 2. Grasshopper script and main components created by authors

scanning toolpath with an expanded FoV. The *device* layer comprises display interfaces, such as monitors and tablet devices, used for visualization and interaction.

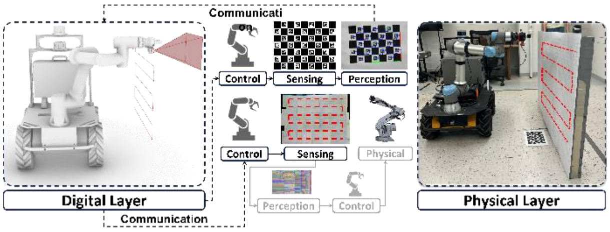

Figure 3. Components for scanning with flexible FoV

4.4.1 Experimental Validation

The proposed workflow was validated through an experiment designed to replicate the full flexible scanning pipeline. A representative 3D printed wall with a height of 40 in (1016 mm), measured from the bottom of the UGV wheels, was used as the target surface. The mobile robot autonomously navigated to a predefined parking position adjacent to the wall. To quantitatively evaluate the scanned area, a rigid board with a 25mm × 25mm grid pattern was placed to simulate the target wall surface.

The flexible FoV scanning approach was evaluated by measuring the surface area covered by the camera while maintaining a constant depth distance. The results can be directly compared with representative camera configurations reported in the literature, including fixed tripod-mounted cameras and cameras mounted on the extruder using rigid brackets. For consistency across configurations, the camera depth distance was fixed at Z = 250 mm, measured from the camera pinhole to the wall surface.

4.4.2 Camera Configuration

An Intel RealSense D435i depth camera was mounted near the UR5e end effector and calibrated in a fixed relative pose. The tool center point (TCP) was defined at the RGB camera pinhole. Although the depth sensor was used for marker detection and localization refinement, only the RGB sensor was used during wall scanning.

The camera was configured with an RGB8 pixel format at a resolution of 1920 × 1080 pixels. The horizontal and vertical fields of view were 69.40° (HFoV) and 42.50° (VFoV), respectively. A frame rate of 30 fps was selected to reduce latency and prevent frame loss along the boundaries of the scanned grid.

Intrinsic camera parameters, including focal length and principal point, were computed using the RealSense SDK in Python. In addition, the physical location of the RGB pinhole relative to the camera housing—including the depth and lateral offsets from the camera centerline—was obtained from the D435i datasheets and incorporated into the digital model. These parameters are summarized in Table 1 and were used consistently throughout the experiment.

Table 1. RGB camera values

Description	Value
Focal Length (*f*)	1.88 mm
Focal Length (*fx, fy*)	1358.17, 1357.83
Principal Point (*cx, cy*)	986.43, 553.09
Depth (*Z*)	250.00 mm
Depth Start Point (*Z′*)	4.20 mm
Pinhole to Centerline (*O*)	32.50 mm

5 Results

Figure 4 illustrates the digital replica of the mobile manipulator, where the RGB sensor pinhole is defined as the TCP for generating the flexible FoV scanning toolpath. The four corner points of the scanned AoI are highlighted. Based on these corner points, the horizontal coverage measured at the bottom edge of the AoI (bottom-left to bottom-right) is 1,193 mm, while the corresponding measurement at the top edge is 1,125 mm. This represents an average width of 1,159mm. The vertical coverage measured along the left edge is 773 mm, and along the right edge, 774 mm, indicating consistent vertical coverage across the scanned area.

The same AoI was independently estimated using the digital model by projecting the camera frustum along the extreme positions of the scanning toolpath. Camera frustums were modeled as Brep pyramids and intersected at a constant depth distance of Z=250 mm, forming a rectangular projected area. Using this approach, the predicted width and height of the scanned area were 1,144 mm and 768 mm, respectively.

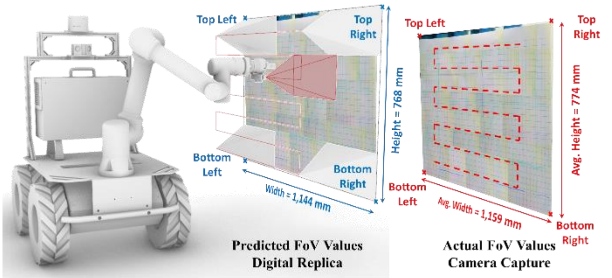

Figure 4. Predicted FoV vs Actual Camera FoV

A quantitative comparison between the measured AoI from the physical experiment and the predicted AoI from the digital replica is summarized in Table 2. The maximum discrepancy in width was 15 mm (1.3%), while the height error was limited to 6 mm (0.8%). These results demonstrate a close agreement between the digital model and the physical experiment, validating a millimetric accuracy of the proposed robotic scanning system in reproducing the predicted AoI. Considering that layer height is typically larger than 10mm, a 6mm error guarantees that the proposed flexible FoV can predict covering all layers in the AoI if a tolerance of an extra layer heigh is incorporated.

Table 2. Camera vs Digital Replica FoV

Frames	Frames Length mm	Avg. Length mm	GH Length mm	Error mm (%)
Bottom	1,193	1,159	1,144	15
Top	1,125			(1.3%)
Left	773	774	768	6
Right	774			(0.8%)

To evaluate the benefits of the proposed flexible FoV scanning approach, its performance was compared against two commonly used alternatives: (1) a fixed FoV camera mounted on a tripod, and (2) a dynamic FoV approach in which a camera is rigidly attached to the printhead and moves along the extrusion path. The comparison metrics include minimum and maximum scanning heights (H_{min}, H_{max}), scanned width (W), scanning time (t), and total scanned area (Ac) for scanning a 3D-printed wall with a height of 1,102mm and a length of 1,144mm.

Unlike fixed or extruder-mounted configurations, the proposed approach dynamically adjusts the scanning toolpath while maintaining a constant depth distance to the wall surface. Although the experiment was conducted on a straight wall, the method is potentially scalable to more complex geometries by preserving a perpendicular viewing direction relative to the surface.

Table 3 summarizes the comparative results. The flexible FoV approach achieved the largest scanned area (0.97 m²), compared to 0.07 m² for the fixed camera and 0.22 m² for the dynamic FoV configuration. This corresponds to an increase in coverage of approximately 13 and 4 times, respectively.

Table 3. Performance metrics comparison: Flexible (proposed method) vs Fixed vs Dynamic FoV

Scenario	Flexible	Fixed	Dynamic
Max Height (H_{max})	1,102 mm	718 mm	1,102 mm
Min Height (H_{min})	334 mm	718 mm	910 mm
Width (W)	1,144 mm	344 mm	1,144 mm
Scanning Time (t)	122.89s	0.03s	10.60s
Area Covered (A_C)	0.97 m^2	0.07 m^2	0.22 m^2

For all scenarios, the depth distance was kept constant at 250 mm, and the scanning speed (for both flexible scanning and printing) was set to 100 mm/s. At this depth, the camera achieved a spatial resolution of 5.55 pixels per millimeter (ppm) across all cases. However, to obtain the same horizontal coverage (approximately 1,144 mm) using a single static camera placement, the camera would need to be positioned at a depth (Z) of approximately 830 mm, computed as:

$$Z = (W/2)/\tan(HFoV/2) \qquad (1)$$

At this depth, the resulting resolution would decrease to 1.68 ppm, assuming the same camera resolution (1920×1080):

$$PPM = 1920/W \qquad (2)$$

This comparison highlights the key contribution of the proposed approach: substantially expanding FoV coverage while preserving high spatial resolution, which cannot be achieved with fixed or printhead-mounted camera configurations alone that are currently used for inline inspection of 3D printed components.

The measured scanning time for the proposed flexible approach was 122.89 s, closely matching the estimated simulation time of 123.50 s, confirming the reliability of the digital planning framework. The dynamic FoV configuration required approximately 10.60 s for a single pass along the extrusion path, while the fixed camera configuration required only 0.03 s per frame at 30 fps. However, this time metric is not comparable due to differences in area coverage.

Finally, the scanned area was computed using a grid-based reference to convert pixel measurements into metric units. Due to frame-drop limitations at 30 fps, minor blind spots occurred near the lateral boundaries of the AoI during flexible scanning, resulting in non-ideal full-perimeter coverage. In addition, the selected frame minimizes lateral overlap (i.e., less than 40%), which could be beneficial when streaming down to a computer vision algorithm to reduce computational load. Despite these limitations, the proposed flexible FoV approach achieved an effective scanned area of 0.97 m², significantly outperforming the fixed and dynamic alternatives.

6 Discussion

The proposed workflow demonstrated the ability to scan a substantially broader AoI of 3D printed wall while maintaining close proximity to the inspected surface and high spatial resolution. Experimental results showed that the measured scanned area closely aligns with the area predicted by the digital model, with only minor discrepancies, confirming the geometric accuracy of the proposed flexible FoV strategy.

Given the selected frame rate of 30 fps, the resulting lateral overlap between consecutive frames was below 40%, which is generally not recommended for image-stitching applications such as panorama or mosaic generation, particularly on low-texture or repetitive surfaces like concrete. This effect is further influenced by the close depth distance (250 mm), high image resolution (1920 × 1080), and robot travel speed (100 mm/s), which collectively result in approximately 6–7 images per vertical strip. However, if proper stitching is desired reducing manipulator speed or resolution, or increasing frame rate will improve the current overlap. It is important to emphasize that the primary objective of the proposed system is inline inspection, rather than image stitching. In this context, close-range imaging is prioritized, and each frame can be analyzed independently to assess surface texture and layer geometry variations without requiring image overlap or mosaicking. Moreover, if downstream perception algorithms are employed for texture or geometric analysis, a lower image acquisition rate may be preferable to reduce computational load while preserving sufficient spatial detail.

Compared to approaches that capture only an instantaneous and localized view near the printhead during extrusion, the proposed parametric scanning strategy requires a longer scanning time. Nevertheless, this additional time enables comprehensive coverage of the printed surface, as the robot scans continuously from bottom to top and then back down from top to bottom. This bidirectional scanning captures information not only from the freshly extruded layers but also from middle and lower layers, which are critical for understanding cumulative deformation, settlement, and load-bearing behavior throughout the printing process.

The comparison between predicted and measured scanned areas showed discrepancies of less than 15 mm in height and 6 mm in width, demonstrating strong alignment between the digital replica and the physical scan and outperforming the methods in the literature. While these results validate the feasibility of the proposed approach, further investigation is required to assess how depth-distance variations may arise when scanning an actual 3D-printed wall with surface irregularities, rather than a flat calibration board. In particular, fluctuations in depth distance can influence scale estimation and pixels-per-millimeter calculations, which are critical parameters for computer vision applications that quantify layer height deviations and geometric defects.

7 Conclusion

This study presented a flexible FoV scanning approach that significantly expands the observable area for inline inspection in 3DCP. The proposed method increases the scanned area by approximately 13 times compared to fixed-camera configurations and 4 times compared to cameras mounted on the printer extruder, while maintaining a close standoff distance from the printed surface and preserving high spatial resolution. By enabling a lateral view of the 3D-printed wall, the approach has potential applications for capturing surface defects, such as cracks and dry material associated with extrudability issues, as well as geometric deformations, including layer height variations, which are critical to buildability assessment.

This research addresses a key limitation in existing inline inspection systems for 3DCP, which predominantly rely on fixed or printhead-mounted cameras with restricted FoV. Previously stated configurations in the literature typically focus on localized, instantaneous observations of freshly extruded material, while overlooking the behavior of lower layers that experience the highest cumulative loading during printing. In contrast, the proposed parametric workflow dynamically updates the camera toolpath based on printing progress, allowing a wider, more representative area of the printed surface to be inspected throughout the build.

Despite its advantages, the proposed workflow also has limitations. The mobile robotic system can navigate to multiple parking positions to scan a printed wall within the printer workspace; however, the proposed stop–scan–move approach limits the scanning while the mobile platform is in motion, since standoff distance will not be fixed. This may reduce inspection continuity in large-scale, fast, and uninterrupted 3DCP operations, particularly when deployed near a stationary gantry. Nevertheless, the scalability of the proposed approach can be achieved by adjusting the standoff distance to increase the effective FoV and reduce the number of required parking locations, and by coordinating inspection frequency with printing parameters such as layer height and deposition speed. The proposed approach remains compatible with both static and mobile robotic arm 3D printing systems, where repositioning is often already part of the operational process.

While having a mobile robot inspector may impose a higher initial cost than a fixed camera setup, it enables autonomous repositioning and optimal camera pose control to achieve high-resolution coverage of the full workpiece, which fixed setups often cannot provide without calibration effort and occlusion issues. In addition, the proposed work envisions a robotic crew operating autonomously without human intervention onsite, while performing multiple tasks (e.g., geometric/thermal monitoring and auxiliary operations [14]), distributing the operational cost into a pull of activities and achieving longer-term higher return on investment, which is critical for operations in remote areas with difficult access

Further real-world testing is recommended to validate performance in active and unstructured onsite 3DCP environments, including consideration of physical constraints. Future research can focus on extending the workflow by integrating a perception layer that analyzes acquired imaging data to detect and predict buildability-related issues, such as layer deformation. This information can then be used to enable proactive interventions and closed-loop control of the 3D printer, advancing toward fully autonomous and intelligent inline inspection systems for 3DCP.

8 Acknowledgements

This study was supported by the FW-HTF award from the National Science Foundation #2128970 and Seed grant from the Purdue Lyles School of Civil and Construction Engineering. Any findings and recommendations in this material are those of the authors and do not necessarily reflect the views of NSF.

References

[1] J. Rojas, A. Braul, and S. Hasanzadeh, "Perceptions of 3D Printing Construction Adoption in Latin America: Opportunities, Barriers, and Strategies for Sustainable Infrastructure," CIB Conferences, vol. 1, no. 1, Jun. 2025, doi: 10.7771/3067-4883.1941.

[2] A. Siddika, M. A. Al Mamun, W. Ferdous, A. K. Saha, and R. Alyousef, "3D-printed concrete: applications, performance, and challenges," *J Sustain Cem Based Mater*, vol. 9, no. 3, pp. 127–164, May 2020, doi: 10.1080/21650373.2019.1705199.

[3] H. Zhao *et al.*, "Realtime and high-accuracy defect monitoring for 3D concrete printing using transformer networks," *Autom Constr*, vol. 170, Feb. 2025, doi: 10.1016/j.autcon.2024.105925.

[4] S. Senthilnathan and B. Raphael, "Predicting Buildability Using the Surface Texture of 3D Printed Concrete Elements," *Journal of Architectural Engineering*, vol. 31, no. 2, Jun. 2025, doi: 10.1061/JAEIED.AEENG-1936.

[5] G. Ma, Y. Li, L. Wang, J. Zhang, and Z. Li, "Realtime quantification of fresh and hardened mechanical property for 3D printing material by intellectualization with piezoelectric transducers," *Constr Build Mater*, vol. 241, Apr. 2020, doi: 10.1016/j.conbuildmat.2019.117982.

[6] K. Mawas, M. Maboudi, and M. Gerke, "A Review on Geometry and Surface Inspection in 3D Concrete Printing," 2025.

[7] K. Banijamali, M. Martin, D. Mascarenas, and A. Kazemian, "Automated Inspection in Robotic 3D Printing: In-Process Geometrical Measurements Using Structured Light Machine Vision," *Journal of Computing in Civil Engineering*, vol. 40, no. 2, Mar. 2026, doi: 10.1061/jccee5.cpeng-7059.

[8] N. An, H. Wang, L. Liu, S. Li, P. Wang, and M. Liu, "Realtime monitoring of extrudability and buildability in 3D concrete printing based on target detection method," *Advances in Structural Engineering*, Jan. 2024, doi: 10.1177/13694332241291247.

[9] R. Mohiuddin, M. C. Policroniades, M. Slepicka, and A. Borrmann, "Optical Process Control for extrusion-based Additive Manufacturing methods in construction," in *ISARC*, 2023.

[10] W. Cui *et al.*, "Geometrical quality inspection in 3D concrete printing using AI-assisted computer vision," *Materials and Structures/Materiaux et Constructions*, vol. 58, no. 2, Mar. 2025, doi: 10.1617/s11527-025-02594-0.

[11] A. Kazemian and B. Khoshnevis, "Realtime extrusion quality monitoring techniques for construction 3D printing," *Constr Build Mater*, vol. 303, Oct. 2021, doi: 10.1016/j.conbuildmat.2021.124520.

[12] X. Yang, O. Lakhal, A. Belarouci, and R. Merzouki, "Automatic Detection and Isolation of Filament Width Deviation during 3-D Printing of Recycled Construction Material," *IEEE/ASME Transactions on Mechatronics*, vol. 29, no. 3, pp. 1939–1948, Jun. 2024, doi: 10.1109/TMECH.2023.3313693.

[13] R. Rill-García *et al.*, "Inline monitoring of 3D concrete printing using computer vision," *Addit Manuf*, vol. 60, Dec. 2022, doi: 10.1016/j.addma.2022.103175.

[14] J. Rojas and S. Hasanzadeh, "Parametric Teleoperation of a Mobile Robot for Placing Printing Supports in 3D Printed Walls," in *ASCE International Conference on Computing in Civil Engineering (i3CE 2025)*, New Orleans, 2025.

[15] J. L. García del Castillo y López, "Machina.NET: A Library for Programming and Realtime Control of Industrial Robots," *J Open Res Softw*, vol. 7, pp. 1–14, 2019, doi: 10.5334/jors.247.

[16] J. Rojas and S. Hasanzadeh, "A Unified Workflow for Enhanced Efficiency in 3D Concrete Printing Using 6DoF Robotic Arm," in *2024 ASCE International Conference on Computing in Civil Engineering*, Pittsburgh, 2024.

[17] J. Rojas and S. Hasanzadeh, "Novel Digital Twin Architecture for 3D Concrete Printing in the AEC Industry," in *Construction Research Congress 2024*, 2024, pp. 1337–1346.